

Brief Communication



Neutrophil Migration Is Mediated by VLA-6 in the Inflamed Adipose Tissue

Hyunseo Lim ¹, Young Ho Choe ¹, Jaeho Lee ¹, Gi Eun Kim ¹,
Jin Won Hyun ², Young-Min Hyun ^{1,*}

¹Department of Anatomy, Brain Korea 21 PLUS Project for Medical Science, Yonsei University College of Medicine, Seoul 03722, Korea

²Department of Biochemistry, Jeju Research Center for Natural Medicine, Jeju National University College of Medicine, Jeju 63243, Korea

OPEN ACCESS

Received: Mar 4, 2024

Revised: May 20, 2024

Accepted: May 26, 2024

Published online: May 31, 2024

*Correspondence to

Young-Min Hyun

Department of Anatomy, Brain Korea 21 PLUS Project for Medical Science, Yonsei University College of Medicine, 50-1 Yonsei-ro, Seodaemun-gu, Seoul 03722, Korea.
Email: ymhyun@yuhs.ac

Copyright © 2024. The Korean Association of Immunologists

This is an Open Access article distributed under the terms of the Creative Commons Attribution Non-Commercial License (<https://creativecommons.org/licenses/by-nc/4.0/>) which permits unrestricted non-commercial use, distribution, and reproduction in any medium, provided the original work is properly cited.

ORCID iDs

Hyunseo Lim 
<https://orcid.org/0009-0001-1063-4942>
Young Ho Choe 
<https://orcid.org/0000-0001-7809-8165>
Jaeho Lee 
<https://orcid.org/0000-0001-7946-0699>
Gi Eun Kim 
<https://orcid.org/0009-0006-6316-1057>
Jin Won Hyun 
<https://orcid.org/0000-0002-3403-3762>
Young-Min Hyun 
<https://orcid.org/0000-0002-0567-2039>

Conflict of Interest

The authors declare no potential conflicts of interest.

ABSTRACT

Adipose tissue, well known for its endocrine function, plays an immunological role in the body. The inflamed adipose tissue under LPS-induced systemic inflammation is characterized by the dominance of pro-inflammatory immune cells, particularly neutrophils. Although migration of macrophages toward damaged or dead adipocytes to form a crown-like structure in inflamed adipose tissue has been revealed, the neutrophilic interaction with adipocytes or the extracellular matrix remains unknown. Here, we demonstrated the involvement of adhesion molecules, particularly integrin $\alpha6\beta1$, of neutrophils in adipocytes or the extracellular matrix of inflamed adipose tissue interaction. These results suggest that disrupting the adhesion between adipose tissue components and neutrophils may govern the accumulation of excessive neutrophils in inflamed tissues, a prerequisite in developing anti-inflammatory therapeutics by inhibiting inflammatory immune cells.

Keywords: Two-photon microscopy; Adipose tissue; Neutrophil; Integrin

INTRODUCTION

The adipose tissue is an endocrine and immunological organ mainly classified into two phenotypes. White adipose tissue (WAT) and brown adipose tissue (BAT) are distributed throughout the body and exhibit distinct characteristics. WAT, comprising white adipocytes, is highly associated with inflammation and is characterized by its energy storage capacity and ability to produce various adipokines. BAT is primarily linked with metabolic functions because of its high mitochondrial concentration (1,2). Anti-inflammatory immune cells, including M2 macrophages, eosinophils, Treg cells, Th2 cells, and innate lymphoid cells (ILCs), help maintain adipose homeostasis. However, the accumulation of pro-inflammatory immune cells, including neutrophils, M1 macrophages, Th1 cells, CD8⁺ T cells, NK cells, ILC1s, and B cells, occurs in the adipose tissue during acute and chronic inflammation. A wide range of immune cells in adipose tissue can regulate acute and chronic immune responses via cytokines (3-5). Most studies have investigated chronic inflammation in adipose tissues, such as obesity. Previous studies have focused on the role of macrophages in inflamed adipose tissue (6-8). However, neutrophil migratory patterns during systemic inflammation in adipose tissues are largely unknown.

Abbreviations

BAT, brown adipose tissue; ECM, cell-extracellular matrix; eWAT, epididymal white adipose tissue; IACUC, Institutional Animal Care and Use Committee; ILC, innate lymphoid cell; PAMP, pathogen-associated molecular patterns; SVF, stromal vascular fraction; VCAM-1, vascular cell adhesion molecule-1; VLA-6, integrin $\alpha 6\beta 1$; WAT, white adipose tissue.

Author Contributions

Conceptualization: Hyun YM; Data curation: Lim H, Choe YH, Lee J, Kim GE, Hyun JW; Formal analysis: Lim H; Funding acquisition: Hyun JW, Hyun YM; Investigation: Lim H; Methodology: Lim H; Project administration: Hyun YM; Validation: Lim H; Visualization: Lim H; Writing - original draft: Lim H; Writing - review & editing: Hyun YM.

LPS, a major outer membrane component of gram-negative bacteria (9,10), leads to a systemic inflammatory environment, such as sepsis (11,12). LPS is recognized by TLR4 through pathogen-associated molecular patterns (PAMP) and activates inflammatory signals (13). Unlike PAMP signals, such as those for LPS, the accumulation of immune cells occurs via damage-associated molecular pattern signals generated from tissue damage or dead cells (14-16). Recruiting appropriate levels of immune cells can induce tissue repair and regeneration. However, excessive accumulation of immune cells attacks the host and promotes inflammation, leading to inflammatory diseases (14,15). In this study, we used LPS to induce systemic inflammation and activate neutrophils, the most abundant immune cell population in the inflamed adipose tissue. Furthermore, laser ablation was employed to induce the directional migration of neutrophils through sterile inflammation. Under these conditions, neutrophils are recruited by various chemoattractants derived from the damaged site (17).

Neutrophils are a type of granulocyte that are the first line of defense during infection and tissue damage (18,19). Neutrophils are produced and released into the bloodstream from the bone marrow. Patrolling neutrophils migrate to the bone marrow, spleen, and liver for elimination after approximately 12 h under homeostatic conditions (20,21). Contrastingly, neutrophils reach the site of inflammation first and start infiltrating the inflamed tissue in inflammatory conditions, such as LPS stimulation (19,22). Additionally, neutrophils are recruited to arterial thrombosis to induce NETosis, which can cause tissue damage (23). In these neutrophil recruitment processes, integrins play a key role in migrating from the interstitial tissues and blood vessels (24). Integrins mediate cell-cell and cell-extracellular matrix (ECM) interactions on the leukocyte surface (25-27). These receptors are heterodimeric proteins comprising α and β subunits (28). Among the integrin receptors expressed in neutrophils, $\beta 1$, $\beta 2$, and $\beta 3$ integrins have a potential for binding with the ECM (29,30). $\beta 1$ integrins mediate cell adhesion to ECM proteins (e.g., laminin, collagen, and fibronectin) and can pair with several α subunits, including $\alpha 2$, $\alpha 4$, $\alpha 5$, $\alpha 6$, and $\alpha 9$ integrins (25,31,32). $\beta 2$ integrins are well known for firm adhesion to vascular endothelium in the process of neutrophil extravasation (33,34). $\beta 3$ integrins have also been demonstrated to mediate binding to ECM, including fibrinogen and fibronectin (35).

Integrin-ligand binding is a critical factor in neutrophil migration. While neutrophils migrate within the inflamed adipose tissue, ECM components such as collagen, laminin, and fibronectin serve as ligands for integrins (25). In addition, both 3T3-L1 cells and primary adipocytes express vascular cell adhesion molecule 1 (VCAM-1), which interacts with integrin $\alpha 4\beta 1$ in a pro-inflammatory environment such as in the presence of TNF (36). Alternately, integrin $\alpha 6\beta 1$, a known representative laminin receptor whose expression can be upregulated by platelet/endothelial cell adhesion molecule-1, is also crucial in the interstitial migration of leukocytes (37). However, the exact integrin-ligand interactions between neutrophils and adipocytes remain unknown. To define the specific integrins required for neutrophil migration in WAT, we performed flow cytometry-based integrin screening and two-photon intravital imaging of epididymal WAT (eWAT) in the presence of an integrin-blocking Ab. Our findings showed that blocking integrins may inhibit excessive neutrophil infiltration into inflamed eWAT, which may help resolve the inflammatory status.

MATERIALS AND METHODS

Animals

C57BL/6 mice were purchased from Orient Bio (Seongnam, South Korea). LysM^{GFP/+} (heterozygous mice) were used to visualize neutrophils. In all experiments, 8–10 wk old male mice were used. All procedures were conducted in accordance with the guidelines of the Institutional Animal Care and Use Committee (IACUC) of Yonsei University College of Medicine and are listed in the animal research proposals (IACUC No. 2022-0116).

Flow cytometry

To induce systemic inflammation, 2.5 mg/kg *Escherichia coli* LPS was injected into male mice, and 1X PBS was injected into the mice as a control. Mice were sacrificed in a CO₂ gas chamber. eWAT was isolated from the mice at different time points. Isolated eWAT was minced with enzyme digestion solution (RPMI 1640 [Welgene, Gyeongsan, Korea] with 20 mM HEPES, without sodium bicarbonate, including 1% fatty acid-free BSA, 50 µg/ml liberase TM [Roche, Basel, Switzerland], and 15 µg/ml DNaseI [Sigma-Aldrich, Burlington, MA, USA]) on the ice. The minced eWAT was incubated for 1 h with shaking at 100 rpm. After incubation, digested eWATs were filtered through a 70-µm strainer with grinding. Next, 3 ml of FACS buffer (1X PBS with 2% FBS and 2 mM EDTA) was added to stop the digestion process. The single-cell suspension was centrifuged at 500×g for 10 min. Floating adipocytes were removed, and the stromal vascular fraction (SVF) was collected. RBCs of SVF were removed using ACK lysis buffer (Gibco, Waltham, MA, USA) and filtered with a 40-µm strainer for single cell isolation. Single cells were blocked with 1 µg purified anti-FcR (CD16/32) Ab (93; BioLegend, San Diego, CA, USA) for 10 min at 4°C. In C57BL/6 mice, neutrophils in SVF cells were stained with 0.5 µg FITC anti-Ly6G (1A8; BioLegend) and 0.2 µg APC anti-CD11b (M1/70; BioLegend) for 30 min at 4°C with light blocked. Conversely, 0.2 µg APC/Cy7 anti-Ly6G (1A8; BioLegend), 0.2 µg PE-Ly6C (HK1.4; BioLegend), 0.2 µg BV711 anti-F4/80 (BM8; BioLegend), and 0.2 µg APC-CD11b (M1/70; BioLegend) were used for staining SVF cells of LysM^{GFP/+} mice. To validate expression of integrins on neutrophils, 0.2 µg PE anti-β1 (HMβ1-1; BioLegend), 0.2 µg PE/Cy7 anti-α2 (HMα2; BioLegend), 0.2 µg PE anti-α4 (R1-2; BioLegend), 0.2 µg PE anti-α5 (HMα5-1; BioLegend), and 0.1 µg PE anti-α6 (GoH3; BioLegend) were used. The following isotype control Abs were used: PE Rat IgG2a, κ (RTK2758; BioLegend), PE Rat IgG2b, κ (RTK4530; BioLegend), and PE or PE/Cy7 Armenian Hamster IgG (HTK888; BioLegend). Flow cytometry was performed using LSRII, FACS Lyric, and Symphony A5 (BD Biosciences, San Jose, CA, USA). Flow cytometric analysis was performed using FlowJo v10.2 (BD Biosciences).

Two-photon intravital imaging

Two-photon intravital microscopy was used to observe neutrophil migration in eWATs *in vivo*. 1X PBS was administered to mice in the control group. To induce systemic inflammation, 2.5 mg/kg of *E. coli* LPS in 1X PBS was injected into the mice in the LPS group. Before *in vivo* imaging, 1X PBS and *E. coli* LPS in 1X PBS were administered through intraperitoneal injections at different time points. For visualizing blood vessels, 50 µg CF[®]405M wheat germ agglutinin (Biotium, Fremont, CA, USA) in 50 µl 1X PBS was injected through intravenous injection before anesthesia. Additionally, to visualize neutrophils in C57BL/6 mice, 5 µg FITC-Ly6G (1A8; BioLegend) was injected intravenously. Zoletil 50 (30 mg/kg; Virbac, Carros, France) and Rompun (10 mg/kg; Bayer, Leverkusen, Germany) were administered. The hair on the mice's abdomen was removed using a hair remover cream. Only portions of the abdominal skin and peritoneum were cut in a circular shape. A cotton swab was used

to expose the eWAT in the abdominal cavity. Exposed eWAT was immersed for 60 min in BODIPY™ dye (Thermo Scientific, Waltham, MA, USA) diluted with 1X PBS at a 1:500 ratio for staining adipocytes. Additionally, the following azide-free low-endotoxin Abs mixed with BODIPY solution were superfused for blocking integrins on neutrophils: anti- β 1 (HM β 1-1; BioLegend), anti- α 4 (R1-2; BioLegend), anti- α 6 (GoH3; BioLegend), Armenian hamster IgG Isotype Ctrl (HTK888; BioLegend), and Rat IgG2a, κ (RTK2758; BioLegend). After all procedures were performed, the mice were placed in a chamber for imaging, and a heating pad was placed on the mouse's body to maintain the body temperature. A 25X water-immersed objective lens was used for all *in vivo* imaging experiments. Four-dimensional imaging videos (512×512 pixels) were recorded with a 1 μ m slice for a depth of 40 μ m. Laser ablation was performed on the adipocytes by adjusting the laser power using the zoom option. Intravital imaging was performed using LSM 7 MP (Zeiss, Oberkochen, Germany) and FVMPE (Olympus, Tokyo, Japan).

Imaging data analysis

The imaging data were analyzed using Volocity v6.3.1 (Quorum, Ontario, Canada) or Imaris v7.2.3 (Bitplane, Belfast, UK). Track velocity (μ m/min), meandering index, and displacement rate (μ m/min) were analyzed through manual tracking with Volocity software. All extravasating or extravasated cells were tracked at least 50 μ m away from the damaged adipocytes. The tracking range was from the edge of the video to the surface of the damaged adipocytes. The trajectory of neutrophil migration was analyzed through spot analysis using the Imaris software and aligned with MATLAB.

Statistical analysis

All statistical analyses were conducted using Prism v7.0 (GraphPad, San Diego, CA, USA). A normality test was performed to select the appropriate test. Following the normality test, data that did not follow a normal distribution curve were analyzed using a nonparametric test. Student's *t*-test or 1-way analysis of variance (ANOVA) with a post hoc test was conducted to compare two or more samples. The average comparison of two independent groups was performed using the Mann–Whitney *U* test. One-way ANOVA was performed to compare the averages of three or more independent groups. *p*-values < 0.05 were considered to indicate statistically significant differences.

RESULTS

LPS-induced systemic inflammation leads to robust neutrophil infiltration into the adipose tissue

We aimed to identify the types of integrins involved in neutrophil migration in adipose tissues. Flow cytometry was used to measure the cell populations. LPS was used to induce an acute inflammatory environment in the eWAT. C57BL/6 and LysM^{GFP/+} mice were used to analyze the innate immune cell population in the eWATs. Neutrophils in the eWAT in the control group were few or nil. About 6 h post LPS inoculation, the infiltrated neutrophil numbers were slightly higher in the eWAT than in the control. However, neutrophil infiltration at 24 h post-LPS inoculation was significantly increased compared to that in the control (**Fig. 1A**). GFP⁺ cells included monocytes, macrophages, and neutrophils in the LysM^{GFP/+} mice (38). Therefore, we classified GFP⁺ cells into neutrophil and non-neutrophil subsets. The non-neutrophil subset was further divided into Ly6C^{low} macrophages, Ly6C^{high} macrophages, and monocytes. Compared with neutrophils in control, the neutrophils

accumulated in the eWAT approximately 24 h after LPS injection were significantly higher in number. In addition, the number of Ly6C^{high} macrophages and monocytes significantly increased 24 h after LPS injection compared to that in the control group. Conversely, Ly6C^{low} macrophages were reduced 24 h after LPS injection compared to those in the control. However, the notable changes in cell numbers of neutrophils, Ly6C^{low} macrophages, Ly6C^{high} macrophages, and monocytes were not observed between 6 and 24 h post LPS injection (Fig. 1B and C). Although Ly6C^{low} macrophages maintain immune homeostasis, Ly6C^{high} macrophages are enriched during acute inflammation and secrete several pro-inflammatory

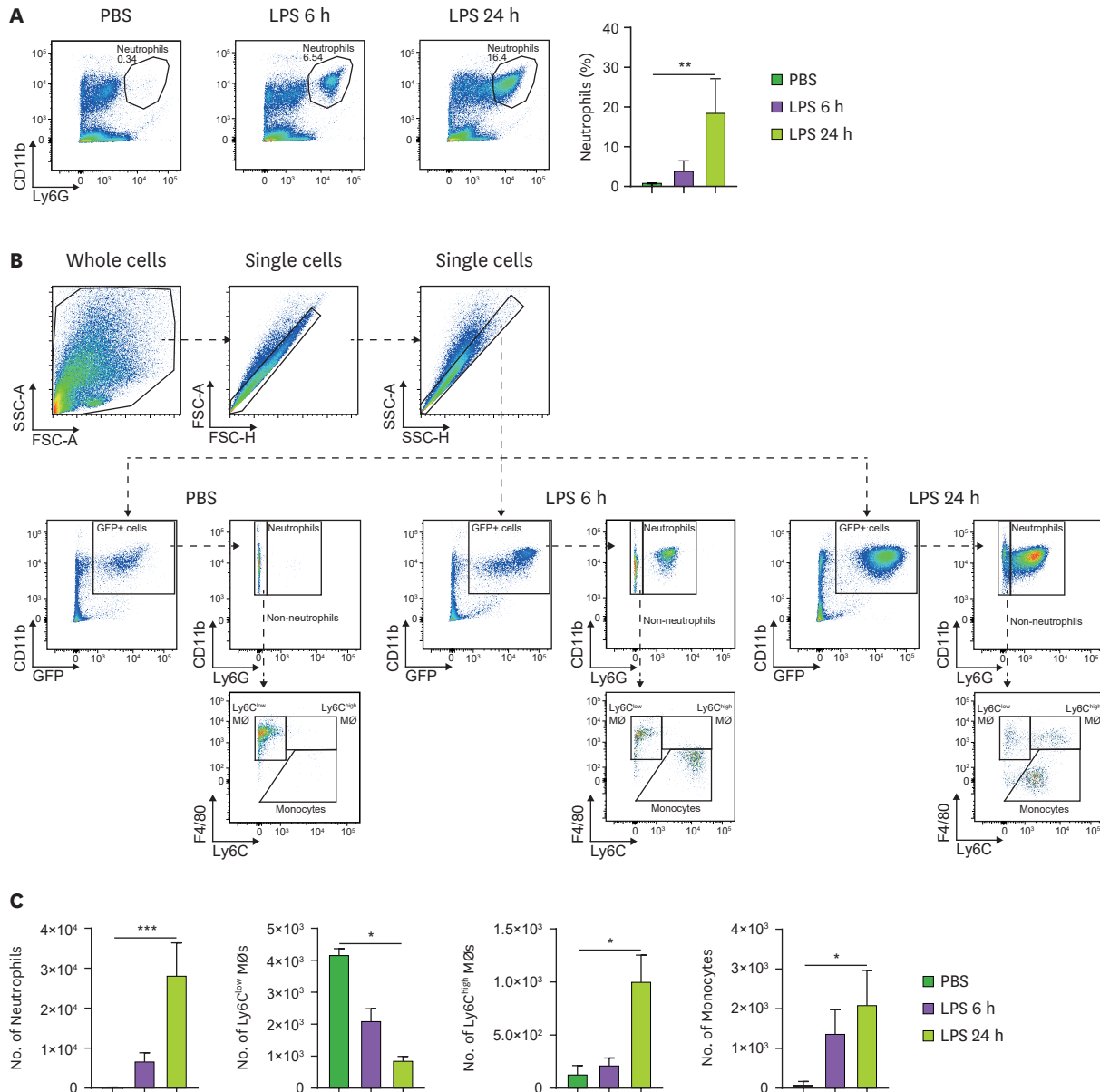


Figure 1. LPS-induced systemic inflammation gradually increases the neutrophil population of inflamed eWAT. (A) Representative scatter plot of neutrophils in eWAT obtained from C57BL/6 male mice. The bar graph of neutrophil percentage in non-inflamed and inflamed eWAT. The neutrophil percentage is calculated by dividing the number of neutrophils by the total number of singlets. (B) Gating strategy of neutrophils in eWAT obtained from LysM^{GFP/+} male mice and representative scatter plot for each condition. (C) The bar graphs of the absolute number of GFP⁺ neutrophils, Ly6C^{low} macrophages, Ly6C^{high} macrophages, and monocytes. Data are presented as the mean±standard deviation. Statistical significance is indicated with an asterisk. *p<0.05, **p<0.01, ***p<0.001.

cytokines (39). These data suggest that compared with 6 h after LPS injection, 24 h after LPS injection induces excessive accumulation of neutrophils, potentially forming a pro-inflammatory condition. Moreover, an increase in the number of Ly6C^{high} macrophages and monocytes indicated that an acute inflammatory response occurred 24 h after LPS injection, contrary to that 6 h after injection.

The motility of neutrophils shows no significant difference between the non-inflamed and inflamed eWAT

We used two-photon microscopy to explore the migratory patterns of neutrophils in non-inflamed and inflamed eWAT within the interstitial tissue. Based on the imaging data, we quantified the number of infiltrating neutrophils in the PBS and LPS groups. Our flow cytometry results showed that the neutrophil population notably increased in eWAT during LPS-induced systemic inflammation. Few neutrophils were observed in the interstitial tissue of the PBS group (Fig. 2A and Supplementary Video 1); contrarily, more neutrophils were present in the interstitial tissue in the inflamed eWAT. The number of neutrophils was significantly higher in the LPS group than in the PBS group (Fig. 2B). However, the migratory patterns of neutrophils were similar in the PBS and LPS groups. In addition, the cell-tracking analysis for each condition showed that the velocity and meandering index were not significantly different between the PBS and LPS groups (Fig. 2C and D). Concurrently, *in vivo* imaging revealed that neutrophils were recruited considerably at 24 h after LPS injection. However, no difference in neutrophil motility was observed between the non-inflamed and inflamed eWAT.

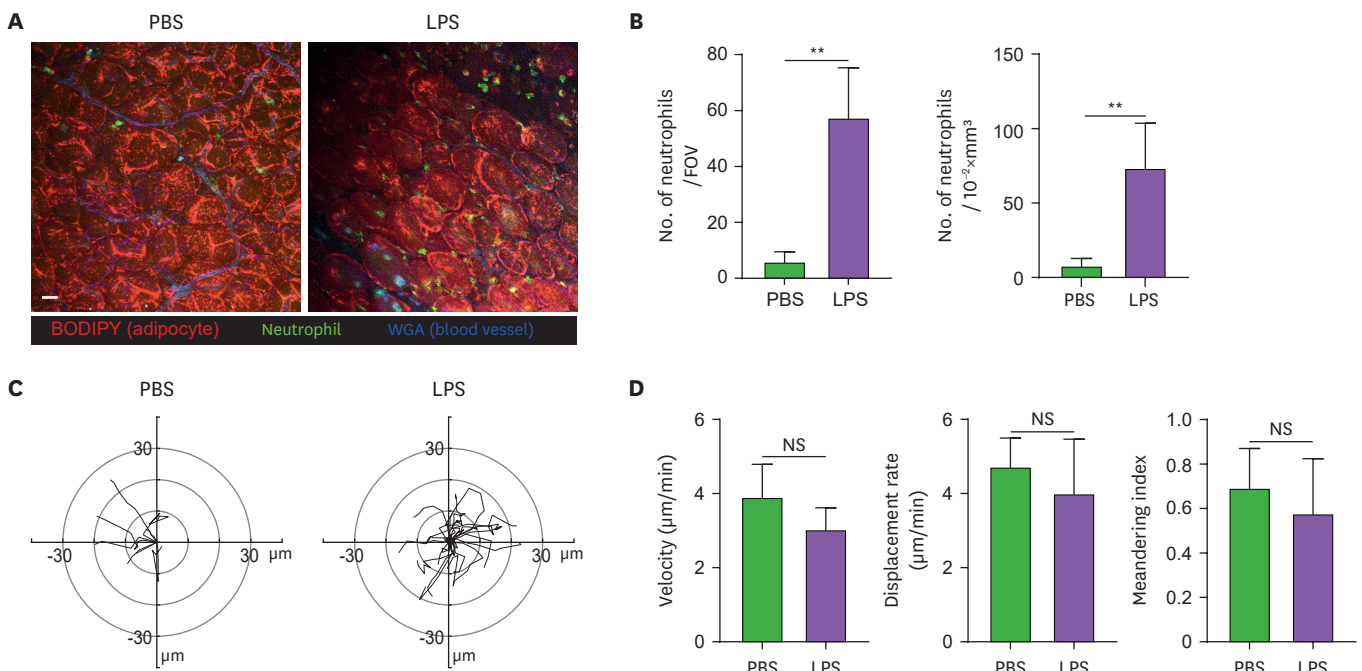


Figure 2. Migratory pattern is not different between neutrophils in non-inflamed and inflamed eWAT. (A) Representative two-photon intravital imaging of eWAT. Neutrophils (green) and blood vessels (blue) are stained with FITC-Ly6G and WGA, respectively. BODIPY red is used for staining adipocytes (red). Scale bar: 30 μm. (B) Neutrophil counts in non-inflamed and inflamed eWAT. The counted neutrophils are converted to the number per unit volume. (C) Migratory paths of neutrophils in non-inflamed eWAT (PBS) and inflamed eWAT (LPS) for 10 min of imaging. The gap between gray circles indicates 10 μm. Randomly selected tracked neutrophils (black lines). (D) The bar graph of velocity, displacement rate, and meandering index of interstitial neutrophils. Velocity, displacement rate, and meandering index are measured by manual cell tracking in eWAT intravital imaging data. Data are presented as the mean±standard deviation. Statistical significance is indicated with an asterisk.

NS, not significant.

**p<0.01.

Blocking of $\beta 1$ integrins inhibits the directionality of neutrophil migration toward the damaged site

Next, we monitored the expression patterns of integrins in neutrophils using flow cytometry. We ascertained specific integrin expression in neutrophils of inflamed eWAT 24 h after LPS injection. Neutrophils expressed $\beta 1$ integrins and their heterodimers, $\alpha 4$, and $\alpha 6$ integrins. Additionally, $\alpha 5$ integrins were also slightly expressed but not $\alpha 2$. (**Fig. 3A**). Hence, we speculated that neutrophils primarily employ $\beta 1$ integrins as a key factor in migration to eWAT. This indicates that neutrophils can migrate to interstitial tissues expressing laminin and VCAM-1. Subsequently, we performed two-photon intravital imaging to confirm that the $\beta 1$ integrin blockade inhibits neutrophil migration to inflamed eWAT. In a previous study, laser-induced sterile injury was used to explore the neutrophil extravascular swarming dynamics (17). We used two-photon laser pulses to induce adipocyte damage to induce directional neutrophil migration during LPS-induced systemic inflammation. After laser ablation, the patterns of neutrophil migration were observed in both isotype control Ab (IgG) and anti- $\beta 1$ integrin blocking Ab (anti- $\beta 1$) treated groups. In the IgG-treated group, the infiltrated neutrophils migrated vigorously toward a single laser-damaged adipocyte. However, in the anti- $\beta 1$ treated group, most of the neutrophils exhibited Brownian motion instead of migrating toward a damaged adipocyte (**Fig. 3B** and **Supplementary Video 2**). The projection of migratory patterns indicates that the migration distance was decreased in the anti- $\beta 1$ treated group compared to that in the IgG-treated group. Additionally, the topical administration of anti- $\beta 1$ caused alterations in the velocity, displacement rate, and meandering index of neutrophils. In the anti- $\beta 1$ treated group, the velocity and directionality of neutrophils were remarkably decreased compared to the IgG-treated group (**Fig. 3C and D**). These results suggest that $\beta 1$ integrin is crucially involved in neutrophil-ECM interactions.

Integrin $\alpha 6\beta 1$ (VLA-6) of neutrophils is crucial to migrate toward damaged adipocyte in inflamed eWAT

In **Fig. 2**, we noted that the blocking of $\beta 1$ integrins inhibits neutrophil motility toward damaged sites within inflamed eWAT. Building upon this finding, our subsequent objective was to elucidate which α subunit of $\beta 1$ integrins with either $\alpha 4$ or $\alpha 6$ subunit influences neutrophil motility within inflamed eWAT. To clarify the roles of $\alpha 4$ and $\alpha 6$ subunits in $\beta 1$ integrins in neutrophil motility, we locally superfused $\alpha 4$ or $\alpha 6$ integrin-blocking Abs on the inflamed eWAT. Subsequently, two-photon intravital microscopy was performed to monitor neutrophil migration. In the IgG-treated group, neutrophils exhibited direct migration toward the laser-damaged site, and a comparable pattern was observed in the group treated with the anti- $\alpha 4$ integrin blocking Ab (anti- $\alpha 4$). The group treated with the anti- $\alpha 6$ integrin blocking Ab (anti- $\alpha 6$) displayed a significantly different migration pattern, characterized by reduced or altered neutrophil movement toward the laser-damaged site (**Fig. 4A** and **Supplementary Video 3**). We presented trajectory paths and assessed their velocity, displacement rate, and meandering index to determine the effects of each Ab on neutrophil motility. The neutrophils in the IgG-treated group exhibited unrestricted mobility, while those treated with anti- $\alpha 4$ displayed partially constrained movement, and only the velocity of neutrophils was significantly diminished. However, the anti- $\alpha 6$ treated group revealed a defective migratory pattern. Velocity, displacement rate, and meandering index were extremely decreased in anti- $\alpha 6$ compared to IgG and anti- $\alpha 4$. Furthermore, neutrophil velocity, displacement rate, and the meandering index markedly declined in the anti- $\alpha 6$ treated group compared to the anti- $\alpha 4$ treated group (**Fig. 4B and C**). To clarify whether neutrophil migration to the laser-damaged site is dependent on $\alpha 6$ integrin, we additionally performed two-photon intravital imaging in inflamed eWAT without laser ablation. Both

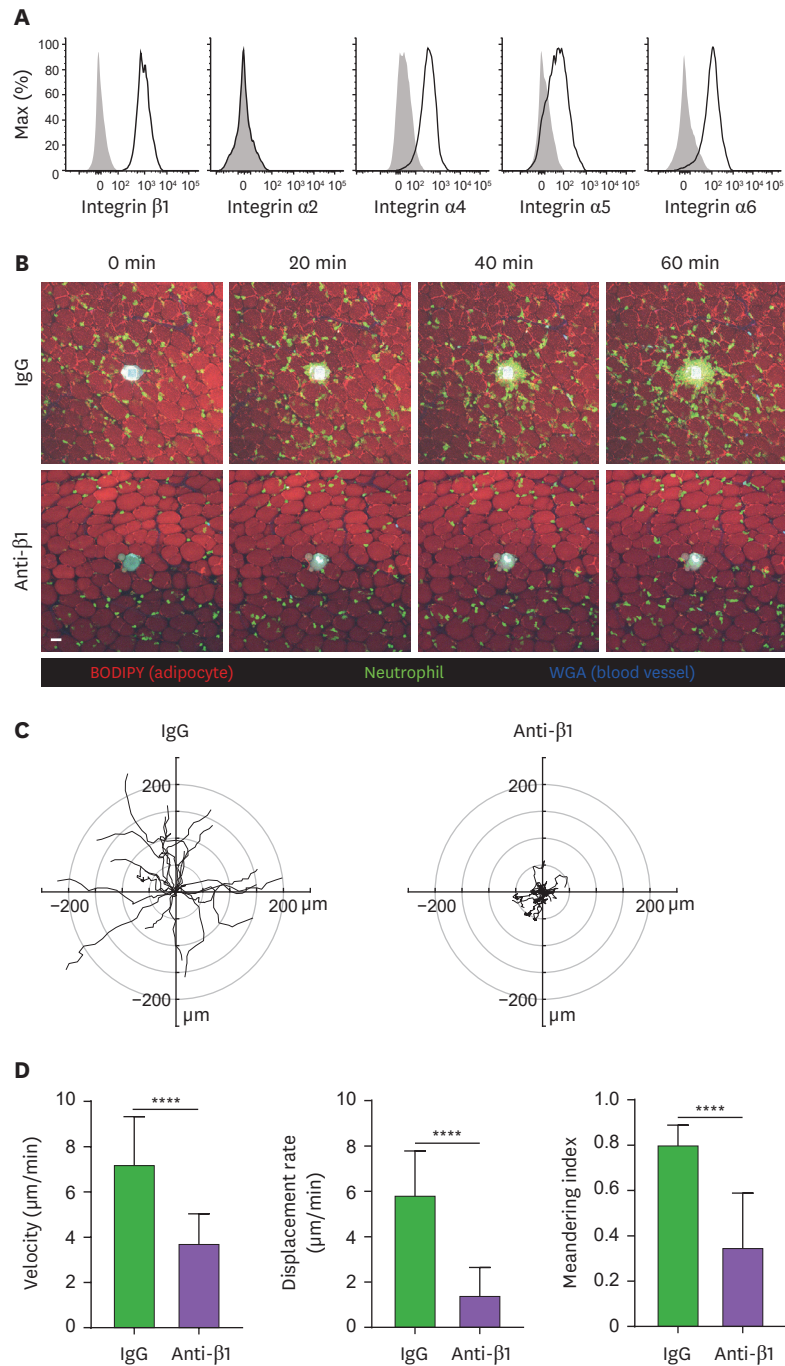


Figure 3. The role of $\beta 1$ integrin in neutrophil migration is related to directional migration toward the damaged site. (A) Integrin expression (black lines) by neutrophils in inflamed eWAT; gray shaded curves, stained with isotype control Ab. (B) Representative two-photon intravital imaging of inflamed eWAT. Laser burning is given to a single adipocyte to induce sterile inflammation. The laser burning site is shown in white color (scale bar: 30 μm). Isotype control Ab (IgG; 50 μg) and anti- $\beta 1$ integrin Ab (Anti- $\beta 1$; 50 μg) are used for functional assay. (C) Migratory paths of neutrophils in inflamed eWAT for 60 min of imaging during which the IgG or anti- $\beta 1$ Ab is topically superfused. The gap between gray circles indicates 50 μm . Randomly selected tracked neutrophils (black lines). (D) Velocity, displacement rate, and meandering index of interstitial neutrophils are measured by manual cell tracking in inflamed eWAT. Data are presented as the mean \pm standard deviation. Statistical significance is indicated with an asterisk. **** $p < 0.0001$.

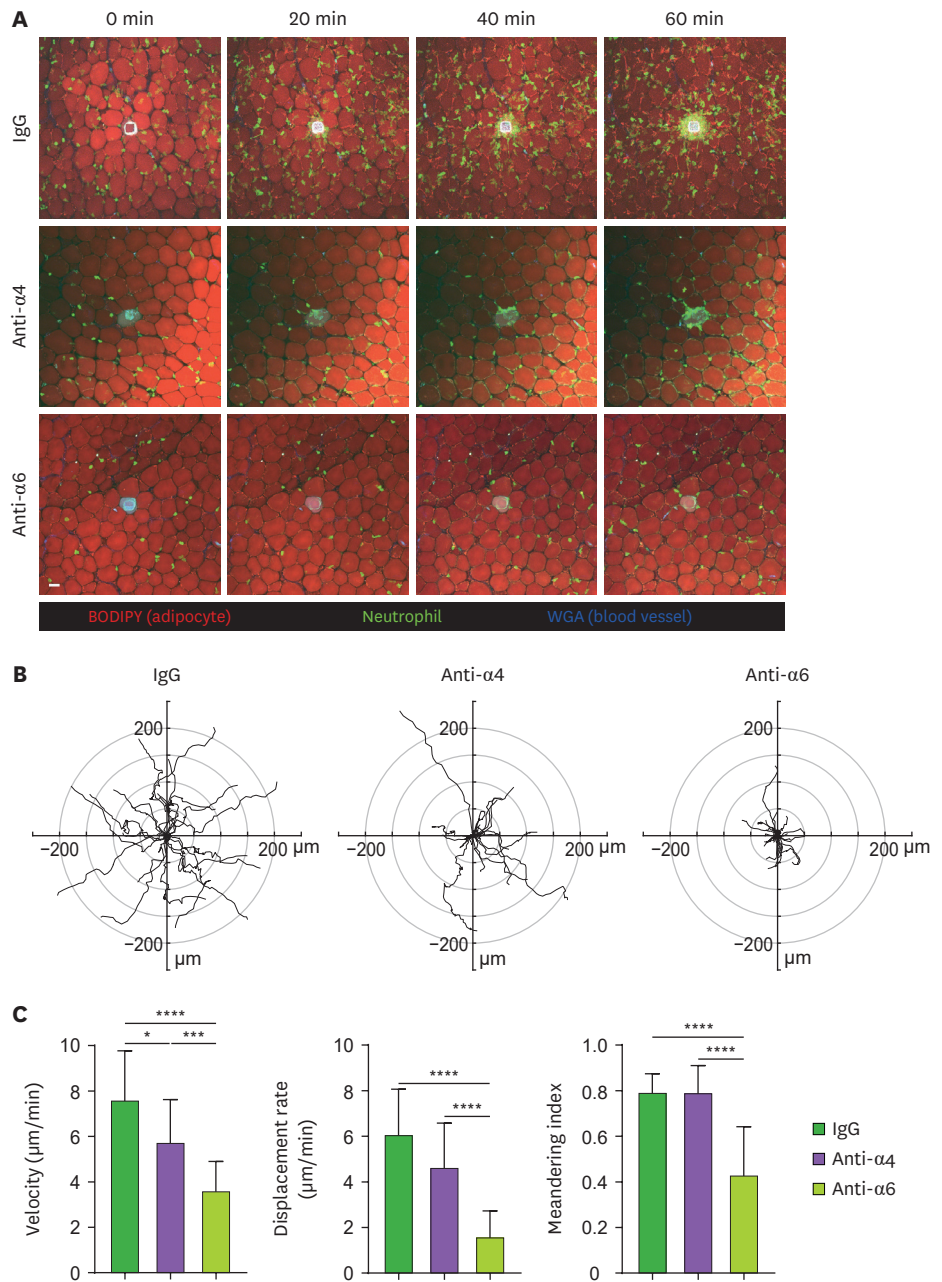


Figure 4. $\alpha 6$ integrin of neutrophil is crucial in migration toward damaged adipocytes. (A) Representative two-photon intravital imaging of inflamed eWAT. Laser burning is given to a single adipocyte. The laser burning site is shown in white color (scale bar: 30 μm). Isotype control Ab (IgG; 100 μg), anti- $\alpha 4$ integrin Ab (anti- $\alpha 4$; 100 μg), and anti- $\alpha 6$ integrin Ab (anti- $\alpha 6$; 100 μg) are used for functional assay. (B) Neutrophil migratory paths are tracked for 60 min in imaging video, during which IgG, anti- $\alpha 4$, or anti- $\alpha 6$ Abs are topically superfused. The gap between gray circles indicates 50 μm . Randomly selected tracked neutrophils (black lines). (C) Velocity, displacement rate, and meandering index of interstitial neutrophils are measured by manual cell tracking in inflamed eWAT. Data are presented as the mean \pm standard deviation. Statistical significance is indicated with an asterisk. * $p < 0.05$, *** $p < 0.001$, **** $p < 0.0001$.

the IgG-treated group and the anti- $\alpha 6$ treated group showed similar migratory patterns of infiltrated neutrophils (Supplementary Fig. 1A and B, Supplementary Video 4). The velocity of neutrophils had no difference in the IgG-treated group compared to the anti- $\alpha 6$ treated group. However, displacement rate and meandering index slightly increased in the anti- $\alpha 6$

treated group (**Supplementary Fig. 1C**). Significant impairment of directional migration toward the laser-damaged site was evident through the neutrophil trajectory (**Fig. 4B** and **Supplementary Fig. 1B**). As previously mentioned, laminin is a component of the ECM complex in the adipose tissue. Altogether, neutrophils employ integrin $\alpha 6\beta 1$ in inflamed eWAT during interstitial migration toward laser-damaged sites.

DISCUSSION

In the adipose tissue, enriched immune cells sustain homeostasis during inflammation (3,40). Adipose tissue inflammation can be classified as acute or chronic. Previous studies on adipose tissue have mostly focused on chronic inflammation, specifically obesity. M1 macrophages play a crucial role in chronic inflammation in adipose tissue (9,41). Unlike the numerous studies that have addressed chronic inflammation in adipose tissue, research on acute and systemic inflammation in adipose tissue is scarce. In this study, we focused on the migratory patterns of neutrophils during LPS-induced systemic inflammation. To determine whether there is a difference in neutrophil motility between non-inflamed and inflamed epididymal adipose tissue (eWAT), we conducted two-photon intravital imaging using $LysM^{GFP/+}$ and C57BL/6 mice. In the inflamed eWAT, the velocity of neutrophils in LPS-injected C57BL/6 mice was lower than that in IgG-treated $LysM^{GFP/+}$ mice (**Figs. 2D** and **3D**). Anti-Ly6G Abs were used to deplete neutrophils (42). To visualize neutrophils in C57BL/6 mice, we injected a minimal amount of a fluorescent-conjugated Ly6G Ab. Thus, we hypothesized that the visualization of neutrophils using a fluorescent-conjugated Ab would slightly inhibit neutrophil migration.

In systemic inflammation, such as sepsis, the expression of pro-inflammatory adipokines and cytokines is upregulated in the adipose tissue (3,4). Adipokines are cytokines synthesized by adipocytes that have been implicated in the regulation of inflammatory, immune, and metabolic processes. Leptin and resistin are pro-inflammatory adipokines secreted by adipocytes. Leptin plays a crucial role in regulating food intake and energy expenditure. Resistin promotes the induction of pro-inflammatory cytokines and adhesion molecules such as intercellular adhesion molecule-1 and VCAM-1. Both leptin and resistin are also related to the chemotaxis of leukocytes and the induction of pro-inflammatory cytokines such as TNF, IL-1 β , and IL-6 (43,44). Cytokines and adipokines induce the accumulation of immune cells in inflamed tissues. Excessive accumulation of immune cells in tissues can damage the host; however, the appropriate recruitment of immune cells can repair and regenerate tissues (14). Especially, it has been reported that macrophages form crown-like structures around damaged or dead adipocytes in inflamed tissue (5). However, the effect of neutrophils that accumulate around damaged or dead adipocytes in systemic inflammation, such as sepsis, has not been extensively studied. Therefore, we intended to mimic adipocyte cell damage or cell death induced by laser ablation in inflamed eWAT using two-photon intravital microscopy (45). We observed numerous neutrophils swarming toward a single damaged or dead adipocyte in real-time. Accordingly, we aimed to identify specific integrin-ligand interactions between eWAT and neutrophils in inflamed eWAT.

The interaction between integrins and ligands is a vital step in immune cell migration (37). During interstitial migration, neutrophils employ $\beta 1$ integrin. $\beta 1$ integrin is highly expressed not only on T lymphocytes but also on neutrophils (27,30). However, the integrin that can prevent excessive accumulation of neutrophils in eWAT is unknown. We focused

on the $\beta 1$ integrin that is involved in interstitial migration. To identify which α subunits form a heterodimer with $\beta 1$ integrin, we conducted flow cytometry. Expression of $\alpha 4$ and $\alpha 6$ integrins is increased in neutrophils from inflamed eWAT. In adipose tissue, VCAM-1 and the ECM, including collagen, laminin, and fibronectin, are ligands for VLA-4 and VLA-6 (25). In a pro-inflammatory environment, the expression of VCAM-1 in adipocytes is upregulated by TNF (36). Our investigation confirmed that $\beta 1$ integrin is essential for neutrophil migration in inflamed adipose tissue. Two-photon intravital imaging showed that blocking $\beta 1$ integrin caused Brownian migration in neutrophils but not amoeboid migration. Furthermore, using *in vivo* imaging, we demonstrated that blocking $\alpha 6$ integrin affected neutrophil motility. In future studies on this process, additional experiments may be necessary to determine whether adipokines, such as leptin or resistin, impact the chemotaxis of neutrophils toward a single damaged or dead adipocyte. Moreover, investigating neutrophil VLA-6 expression in the adipose tissue of obese mice is essential for understanding chronic inflammation. Through this investigation of integrins on neutrophils, we anticipate being able to propose new directions for research into the treatment of diseases, such as systemic inflammatory response syndrome or sepsis-associated acute kidney injury (46-48).

ACKNOWLEDGEMENTS

This study was supported by the faculty research grant of Yonsei University College of Medicine (6-2023-0081 to Y.M.H) and the National Research Foundation funded by the Ministry of Science and ICT (MSIT) of the Government of Korea (RS-2023-00207834 to Y.-M.H.) and the Ministry of Education (RS-2023-00270936 to J.W.H).

SUPPLEMENTARY MATERIALS

Supplementary Figure 1

The $\alpha 6$ integrin blocking Ab has minimal impact on the random migration of infiltrated neutrophils in inflamed eWAT. (A) Representative two-photon intravital imaging of inflamed eWAT. Isotype control Ab (IgG; 100 μ g) and anti- $\alpha 6$ integrin Ab (anti- $\alpha 6$; 100 μ g) were used for functional assay. (B) The migratory path of neutrophils is monitored in a 60 min imaging video, during which IgG or anti- $\alpha 6$ Abs is applied topically. The gap between gray circles indicates 50 μ m. Randomly selected tracked neutrophils (black lines). (C) Velocity, displacement rate, and meandering index of infiltrated neutrophils in inflamed eWAT are quantified through manual tracking. Data are presented as the mean \pm standard deviation. Statistical significance is indicated with an asterisk.

Supplementary Video 1

Neutrophil migration in non-inflamed and inflamed eWAT of C57BL/6 mice.

Supplementary Video 2

The blocking Ab to $\beta 1$ integrin inhibits neutrophil migration toward a damaged adipocyte.

Supplementary Video 3

The blocking Ab to $\alpha 6$ integrin inhibits neutrophil migration toward a damaged adipocyte.

Supplementary Video 4

The blocking Ab to $\alpha 6$ integrin has no effect on neutrophil migration within inflamed eWAT.

REFERENCES

1. Harms M, Seale P. Brown and beige fat: development, function and therapeutic potential. *Nat Med* 2013;19:1252-1263. [PUBMED](#) | [CROSSREF](#)
2. Choe SS, Huh JY, Hwang IJ, Kim JI, Kim JB. Adipose tissue remodeling: its role in energy metabolism and metabolic disorders. *Front Endocrinol (Lausanne)* 2016;7:30. [PUBMED](#) | [CROSSREF](#)
3. Man K, Kallies A, Vasanthakumar A. Resident and migratory adipose immune cells control systemic metabolism and thermogenesis. *Cell Mol Immunol* 2022;19:421-431. [PUBMED](#) | [CROSSREF](#)
4. Karampela I, Christodoulatos GS, Dalamaga M. The role of adipose tissue and adipokines in sepsis: inflammatory and metabolic considerations, and the obesity paradox. *Curr Obes Rep* 2019;8:434-457. [PUBMED](#) | [CROSSREF](#)
5. Lindhorst A, Raulien N, Wieghofer P, Eilers J, Rossi FMV, Bechmann I, Gericke M. Adipocyte death triggers a pro-inflammatory response and induces metabolic activation of resident macrophages. *Cell Death Dis* 2021;12:579. [PUBMED](#) | [CROSSREF](#)
6. Chavakis T, Alexaki VI, Ferrante AW Jr. Macrophage function in adipose tissue homeostasis and metabolic inflammation. *Nat Immunol* 2023;24:757-766. [PUBMED](#) | [CROSSREF](#)
7. Joffin N, Gliniak CM, Funcke JB, Paschoal VA, Crewe C, Chen S, Gordillo R, Kusminski CM, Oh DY, Geldenhuys WJ, et al. Adipose tissue macrophages exert systemic metabolic control by manipulating local iron concentrations. *Nat Metab* 2022;4:1474-1494. [PUBMED](#) | [CROSSREF](#)
8. Park CS, Shastri N. The role of T cells in obesity-associated inflammation and metabolic disease. *Immune Netw* 2022;22:e13. [PUBMED](#) | [CROSSREF](#)
9. Page MJ, Kell DB, Pretorius E. The role of lipopolysaccharide-induced cell signalling in chronic inflammation. *Chronic Stress (Thousand Oaks)* 2022;6:24705470221076390. [PUBMED](#) | [CROSSREF](#)
10. Poggi M, Bastelica D, Gual P, Iglesias MA, Gremaux T, Knauf C, Peiretti F, Verdier M, Juhan-Vague I, Tanti JF, et al. C3H/HeJ mice carrying a toll-like receptor 4 mutation are protected against the development of insulin resistance in white adipose tissue in response to a high-fat diet. *Diabetologia* 2007;50:1267-1276. [PUBMED](#) | [CROSSREF](#)
11. Hung YL, Fang SH, Wang SC, Cheng WC, Liu PL, Su CC, Chen CS, Huang MY, Hua KF, Shen KH, et al. Corylin protects LPS-induced sepsis and attenuates LPS-induced inflammatory response. *Sci Rep* 2017;7:46299. [PUBMED](#) | [CROSSREF](#)
12. Byun DJ, Lee J, Yu JW, Hyun YM. NLRP3 exacerbate NETosis-associated neuroinflammation in an LPS-induced inflamed brain. *Immune Netw* 2023;23:e27. [PUBMED](#) | [CROSSREF](#)
13. Kawai T, Akira S. The role of pattern-recognition receptors in innate immunity: update on toll-like receptors. *Nat Immunol* 2010;11:373-384. [PUBMED](#) | [CROSSREF](#)
14. Gong T, Liu L, Jiang W, Zhou R. DAMP-sensing receptors in sterile inflammation and inflammatory diseases. *Nat Rev Immunol* 2020;20:95-112. [PUBMED](#) | [CROSSREF](#)
15. Piccinini AM, Midwood KS. DAMPening inflammation by modulating TLR signalling. *Mediators Inflamm* 2010;2010:672395. [PUBMED](#) | [CROSSREF](#)
16. Vénéreau E, Ceriotti C, Bianchi ME. Damps from cell death to new life. *Front Immunol* 2015;6:422. [PUBMED](#) | [CROSSREF](#)
17. Lämmermann T, Afonso PV, Angermann BR, Wang JM, Kastenmüller W, Parent CA, Germain RN. Neutrophil swarms require LTB4 and integrins at sites of cell death in vivo. *Nature* 2013;498:371-375. [PUBMED](#) | [CROSSREF](#)
18. de Oliveira S, Rosowski EE, Huttenlocher A. Neutrophil migration in infection and wound repair: going forward in reverse. *Nat Rev Immunol* 2016;16:378-391. [PUBMED](#) | [CROSSREF](#)
19. Kolaczowska E, Kubes P. Neutrophil recruitment and function in health and inflammation. *Nat Rev Immunol* 2013;13:159-175. [PUBMED](#) | [CROSSREF](#)
20. Nicolás-Ávila JA, Adrover JM, Hidalgo A. Neutrophils in homeostasis, immunity, and cancer. *Immunity* 2017;46:15-28. [PUBMED](#) | [CROSSREF](#)
21. Hidalgo A, Chilvers ER, Summers C, Koenderman L. The neutrophil life cycle. *Trends Immunol* 2019;40:584-597. [PUBMED](#) | [CROSSREF](#)

22. Margraf A, Lowell CA, Zarbock A. Neutrophils in acute inflammation: current concepts and translational implications. *Blood* 2022;139:2130-2144. [PUBMED](#) | [CROSSREF](#)
23. Cha MJ, Ha J, Lee H, Kwon I, Kim S, Kim YD, Nam HS, Lee HS, Song TJ, Choi HJ, et al. Neutrophil recruitment in arterial thrombus and characteristics of stroke patients with neutrophil-rich thrombus. *Yonsei Med J* 2022;63:1016-1026. [PUBMED](#) | [CROSSREF](#)
24. Nourshargh S, Hordijk PL, Sixt M. Breaching multiple barriers: leukocyte motility through venular walls and the interstitium. *Nat Rev Mol Cell Biol* 2010;11:366-378. [PUBMED](#) | [CROSSREF](#)
25. Lindbom L, Werr J. Integrin-dependent neutrophil migration in extravascular tissue. *Semin Immunol* 2002;14:115-121. [PUBMED](#) | [CROSSREF](#)
26. Mezu-Ndubuisi OJ, Maheshwari A. The role of integrins in inflammation and angiogenesis. *Pediatr Res* 2021;89:1619-1626. [PUBMED](#) | [CROSSREF](#)
27. Overstreet MG, Gaylo A, Angermann BR, Hughson A, Hyun YM, Lambert K, Acharya M, Billroth-Maclurg AC, Rosenberg AF, Topham DJ, et al. Inflammation-induced interstitial migration of effector CD4⁺ T cells is dependent on integrin α V. *Nat Immunol* 2013;14:949-958. [PUBMED](#) | [CROSSREF](#)
28. Hyun YM, Lefort CT, Kim M. Leukocyte integrins and their ligand interactions. *Immunol Res* 2009;45:195-208. [PUBMED](#) | [CROSSREF](#)
29. Blythe EN, Weaver LC, Brown A, Dekaban GA. Beta2 integrin CD11d/CD18: from expression to an emerging role in staged leukocyte migration. *Front Immunol* 2021;12:775447. [PUBMED](#) | [CROSSREF](#)
30. Werr J, Xie X, Hedqvist P, Ruoslahti E, Lindbom L. Beta1 integrins are critically involved in neutrophil locomotion in extravascular tissue in vivo. *J Exp Med* 1998;187:2091-2096. [PUBMED](#) | [CROSSREF](#)
31. Riopel MM, Li J, Liu S, Leask A, Wang R. β 1 integrin-extracellular matrix interactions are essential for maintaining exocrine pancreas architecture and function. *Lab Invest* 2013;93:31-40. [PUBMED](#) | [CROSSREF](#)
32. Brakebusch C, Fässler R. beta 1 integrin function in vivo: adhesion, migration and more. *Cancer Metastasis Rev* 2005;24:403-411. [PUBMED](#) | [CROSSREF](#)
33. Hyun YM, Choe YH, Park SA, Kim M. LFA-1 (CD11a/CD18) and Mac-1 (CD11b/CD18) distinctly regulate neutrophil extravasation through hotspots I and II. *Exp Mol Med* 2019;51:1-13. [PUBMED](#) | [CROSSREF](#)
34. Hyun YM, Sumagin R, Sarangi PP, Lomakina E, Overstreet MG, Baker CM, Fowell DJ, Waugh RE, Sarelius IH, Kim M. Uropod elongation is a common final step in leukocyte extravasation through inflamed vessels. *J Exp Med* 2012;209:1349-1362. [PUBMED](#) | [CROSSREF](#)
35. Kim HY, Skokos EA, Myer DJ, Agaba P, Gonzalez AL. Alpha(v)beta(3) integrin regulation of respiratory burst in fibrinogen adherent human neutrophils. *Cell Mol Bioeng* 2014;7:231-242. [PUBMED](#) | [CROSSREF](#)
36. Chung KJ, Chatzigeorgiou A, Economopoulou M, Garcia-Martin R, Alexaki VI, Mitroulis I, Nati M, Gebler J, Ziemssen T, Goelz SE, et al. A self-sustained loop of inflammation-driven inhibition of beige adipogenesis in obesity. *Nat Immunol* 2017;18:654-664. [PUBMED](#) | [CROSSREF](#)
37. Luster AD, Alon R, von Andrian UH. Immune cell migration in inflammation: present and future therapeutic targets. *Nat Immunol* 2005;6:1182-1190. [PUBMED](#) | [CROSSREF](#)
38. Kreisel D, Nava RG, Li W, Zinselmeyer BH, Wang B, Lai J, Pless R, Gelman AE, Krupnick AS, Miller MJ. In vivo two-photon imaging reveals monocyte-dependent neutrophil extravasation during pulmonary inflammation. *Proc Natl Acad Sci U S A* 2010;107:18073-18078. [PUBMED](#) | [CROSSREF](#)
39. Yao W, Chen Y, Li Z, Ji J, You A, Jin S, Ma Y, Zhao Y, Wang J, Qu L, et al. Single cell RNA sequencing identifies a unique inflammatory macrophage subset as a druggable target for alleviating acute kidney injury. *Adv Sci (Weinh)* 2022;9:e2103675. [PUBMED](#) | [CROSSREF](#)
40. Grant RW, Dixit VD. Adipose tissue as an immunological organ. *Obesity (Silver Spring)* 2015;23:512-518. [PUBMED](#) | [CROSSREF](#)
41. Catrysse L, van Loo G. Adipose tissue macrophages and their polarization in health and obesity. *Cell Immunol* 2018;330:114-119. [PUBMED](#) | [CROSSREF](#)
42. Boivin G, Faget J, Ancy PB, Gkasti A, Mussard J, Engblom C, Pflirschke C, Contat C, Pascual J, Vazquez J, et al. Durable and controlled depletion of neutrophils in mice. *Nat Commun* 2020;11:2762. [PUBMED](#) | [CROSSREF](#)
43. Jiang S, Park DW, Tadie JM, Gregoire M, Deshane J, Pittet JF, Abraham E, Zmijewski JW. Human resistin promotes neutrophil proinflammatory activation and neutrophil extracellular trap formation and increases severity of acute lung injury. *J Immunol* 2014;192:4795-4803. [PUBMED](#) | [CROSSREF](#)
44. Souza-Almeida G, D'Avila H, Almeida PE, Luna-Gomes T, Liechocki S, Walzog B, Hepper I, Castro-Faria-Neto HC, Bozza PT, Bandeira-Melo C, et al. Leptin mediates in vivo neutrophil migration: involvement of tumor necrosis factor-alpha and cxcl1. *Front Immunol* 2018;9:111. [PUBMED](#) | [CROSSREF](#)
45. McDonald B, Pittman K, Menezes GB, Hirota SA, Slaba I, Waterhouse CC, Beck PL, Muruve DA, Kubes P. Intravascular danger signals guide neutrophils to sites of sterile inflammation. *Science* 2010;330:362-366. [PUBMED](#) | [CROSSREF](#)

46. Wolf D, Anto-Michel N, Blankenbach H, Wiedemann A, Buscher K, Hohmann JD, Lim B, Bäuml M, Marki A, Mauler M, et al. A ligand-specific blockade of the integrin Mac-1 selectively targets pathologic inflammation while maintaining protective host-defense. *Nat Commun* 2018;9:525. [PUBMED](#) | [CROSSREF](#)
47. Yuki K, Hou L. Role of beta2 integrins in neutrophils and sepsis. *Infect Immun* 2020;88:e00031-20. [PUBMED](#) | [CROSSREF](#)
48. Kwak SH, Ahn S, Shin MH, Leem AY, Lee SH, Chung K, Kim YS, Lee SG, Park MS. Identification of biomarkers for the diagnosis of sepsis-associated acute kidney injury and prediction of renal recovery in the intensive care unit. *Yonsei Med J* 2023;64:181-190. [PUBMED](#) | [CROSSREF](#)